Environmental Earth Sciences (2020) 79:232
https://doi.org/10.1007/s12665-020-08958-9

ORIGINAL ARTICLE

Assessment of gully development using geomorphic change detection between pre- and post-urbanization scenarios

Anesmar Olino de Albuquerque[1] · Osmar Abílio de Carvalho Júnior[1] · Renato Fontes Guimarães[1] · Roberto Arnaldo Trancoso Gomes[1] · Potira Meirelles Hermuche[1]

Received: 29 January 2019 / Accepted: 27 April 2020 / Published online: 14 May 2020

Abstract

Urbanization processes have caused changes in the runoff behavior, especially by impervious surfaces produced by paving and buildings. Impermeable surfaces prevent the infiltration of rainwater, increasing the volume and speed of runoff. Besides, inadequate urban planning coupled with heavy rains promotes the evolution of erosion processes, especially in peri-urban areas. This research aims to identify spatial patterns of geomorphic change in the gully areas due to urbanization in the city of Jacareí (SP). The methodology has the following steps: (1) elaboration of the Digital Elevation Model (DEM) from stereophotogrammetric techniques; (2) elaboration of the pre- and post-urbanization DEM; (3) extraction of contributing area using the D-Infinity method and of the topographic indices (topographic wetness, stream power, and compound topographic); and (4) calculate the difference between the pre- and post-urbanization topographic attributes. The preparation of the pre- and post-urbanization DEM used the MATCH-T DSM and DTMaster modules, both belonging to the INPHO system. Photogrammetric techniques allow the generation of digital models suitable for hydrological studies. The urbanization exposed an evident influence on the triggering of erosion, evidencing an increase of all topographic indices in areas that develop gullies.

Keywords Change detection · Digital elevation model · Erosion · Geomorphometry · Photogrammetry

Introduction

In today's world, more people are living in urban areas than in rural areas, with a global urban population growth that expects to reach 66% by 2015 (United Nations 2015). The metropolitan regions cause global environmental change (Grimmm et al. 2008, Flörke et al. 2018), expanding globally twice as faster as populations (Angel et al. 2011; Seto et al. 2011). Rapid urban growth coupled with poor planning leads to a modification of the hydrological system (e.g., Deng et al. 2015; Deng and Xu 2018; Shukla and Gedam 2019) and lead to accelerated erosion (e.g., Wang et al. 2018; Zolezzi et al. 2018; Jeong and Dorn 2019). The urbanization causes a significant increase in impervious surfaces such as paved roads, roofs, and parking lots, which reduce rainwater infiltration and increase the runoff (Gurnell et al. 2007; Taniguchi et al. 2018). Impervious surface changes the hydrologic system in different ways: (1) modify the drainage network; (2) decrease groundwater recharge; (3) decrease the lag interval between onset of precipitation and the higher runoff peaks; (4) increase the total volume of storm water runoff that in extreme cases could be significantly times greater than under natural conditions; and (5) decrease mean residence time of stream flow (Rose and Peters 2001; Burns et al. 2005). Therefore, runoff concentration from the impermeable areas is one of the main factors for the severe accelerated soil erosion and gully development in the urban landscape (e.g., Bouchnak et al. 2009; Adediji et al. 2011). Many urban gullies result from the following combination of elements: high-volume runoff on steep roads, unpaved

✉ Osmar Abílio de Carvalho Júnior
osmarjr@unb.br

Anesmar Olino de Albuquerque
anesmar_2000@hotmail.com

Renato Fontes Guimarães
renatofg@unb.br

Roberto Arnaldo Trancoso Gomes
robertogomes@unb.br

Potira Meirelles Hermuche
potirahermuche@gmail.com

[1] Departamento de Geografia, Campus Universitário Darcy Ribeiro, Universidade de Brasília (UnB), Asa Norte, Brasília, DF, Brasil

drains, lack of engineering works, and the precarious state of drainage maintenance (Adedeji et al. 2013). Erosion processes decline with the consolidation of the urban landscape (Archibold et al. 2003). However, the peri-urban areas wherein many cities do not have adequate infrastructure are more susceptible to erosion and other environmental impacts (Meija and Moglen 2010; Costa et al. 2018; Pribadi et al. 2018). Moreover, the expansion often occurs in undervalued areas near the steep areas, coastal wetlands, and poorly drained floodplains (Gupta 2002).

Understanding and measuring patterns of accumulation, transport, and deposition of the Earth's surface materials are primary factors to investigate, predict, and mitigate environmental and urban damage. An attractive approach for studying the spatial–temporal behavior of the surface processes is geomorphic change detection (James et al. 2012). The simplest method for geomorphic change detection is the difference between the successive Digital Elevation Model (DEM), which reveals spatial–temporal patterns of volumetric changes. This methodology estimates the rates of change and generates a spatial representation of the geomorphological dynamics. Potentially unstable areas consist of localities with morphological changes. DEM change detection include different geomorphological studies, such as tectonic (e.g., Oskin et al. 2012; Ren et al. 2014), slope processes and mass movement (e.g., Hsieh et al. 2016; Mora et al. 2018; Xiong et al. 2018; Peppa et al. 2019), fluvial (e.g., Grove et al. 2013; Norman et al. 2017; Carrivick and Smith 2019; Kasprak et al. 2019), coastal dunes (e.g., Walker et al. 2013; Duffy et al. 2018; Le Mauff et al. 2018; Guisado-Pintado et al. 2019), glacial (e.g., Nuth and Kääb 2011; Jones et al. 2013; Micheletti et al. 2017; Seier et al. 2017), and karst (e.g., Siart et al. 2009; Carvalho Junior et al. 2013; Kobal et al. 2015).

In this respect, many studies on the evolution of gully systems focus on comparisons of multi-date DEMs to monitor and calculate the volumetric changes (e.g., Cavalli et al. 2017; Balaguer-Puig et al. 2017, 2018). In these studies, the development of DEMs used different techniques: aerial photographs (e.g., Martínez-Casasnovas 2009; Piccarreta et al. 2012; Aucelli et al. 2016), aerial photography from an unmanned aerial vehicle (e.g., Glendell et al. 2017; Pineux et al. 2017; Eltner et al. 2018), airborne and terrestrial laser scanning (e.g., DeLong et al. 2012; Goodwin et al. 2017; Taylor et al. 2018), and smartphone camera (Vinci et al. 2017). The multi-temporal analysis also allows an understanding of the effects of runoff terrain interaction. In search of an adequate indicator of the urban impacts on water flow and gullies, Junior et al. (2010) proposed an accumulated-flow differencing, enabling evaluate the drainage change and the appearance of gullies. The method evidences the runoff effects from urban morphological into a natural area, comparing pre- and post-urbanization scenarios.

The main objective of this study is to evaluate the spatial patterns of geomorphic change caused by urbanization and its effects on gullies in the city of Jacareí. In this context, the research has two secondary objectives: (1) elaboration of the pre- and post-urbanization scenarios from a DEM derived from aerial photographs and digital processing techniques; and (2) change detection analysis considering topographic attributes. In the prediction of the spatial pattern of gullies, we compare the contributing area (A) and three topographic indices: (1) Topographic Humidity Index (W); (2) Flow Power Index (P); and (3) Composite Topographic Index (CTI), also known as Thorne Index. The present research evaluates the difference of terrain attributes in surface runoff and drainage channels, not evaluating the behavior in large rivers that suffer severe anthropogenic changes with constant riverbank movement (Dewan et al 2017; Güneralp and Rhoads 2009).

Study area

The Jacareí municipality is in the eastern part of the São Paulo State, a region known as the Valley of the River Paraiba do Sul (VRPS). The study area has a size of 3.9 km^2, with an average altitude of 580 m between the Mantiqueira and Mar mountain ranges (Fig. 1). The city of Jacarei originated from a small settlement in 1652, changed to condition village in 1653, and became a city only on April 3, 1849. Historically, the urbanization process in the VRPS occurred with railway and highways (Presidente Dutra, Ayrton Senna, Dom Pedro I, and Carvalho Pinto). Jacarei City developed along the Dutra highway, the main road connecting the two largest Brazilian cities (Rio de Janeiro and São Paulo). Jacareí City showed a marked increase in population growth during the period 1940–2010 (IPEADATA 2014), located in a region with sizeable urban conurbation. However, urban growth also occurs in inappropriate areas for urbanization, such as slopes and floodplains.

The VRPS region has a warm subtropical climate with Cwa Köppen classification, containing hot summers, milder winters, and an average annual temperature of 21 ºC. The VRPS region has an average annual rainfall between 1200 and 1300 mm lower than the extended system of mountain ranges: Mantiqueira (1300–2000 mm) and the Serra do Mar (1300–2800 mm) (São Paulo 2006). The highest rainfall regime occurs from December to January with average accumulated rainfall between 200 and 250 mm/month, while the driest period is from May to August with lower rainfall 50 mm/month (Marengo and Alves 2005). Climate dynamic of VRPS do not suffer significant variations due to the presence of mass Tropical Atlantic in most of the year (Conti 1975).

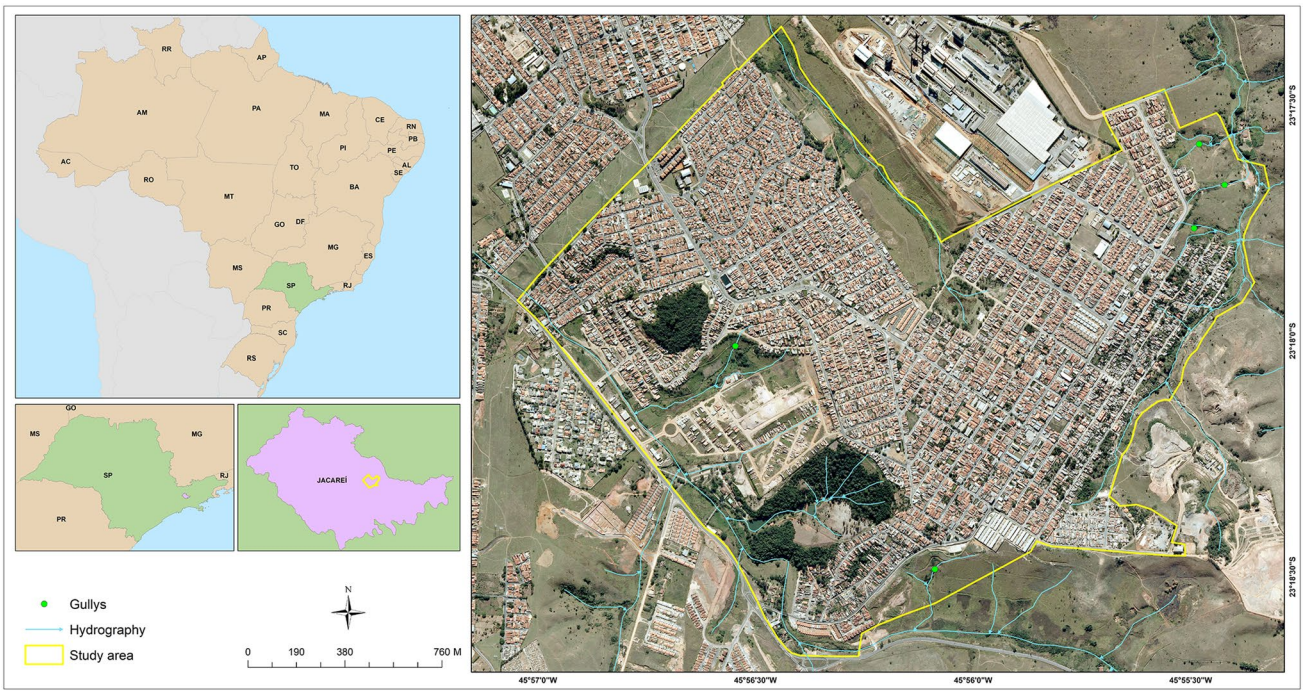

Fig. 1 Study area location

The Taubaté Basin is part of the Continental Rift of Southeastern Brazil, comprising Tertiary sedimentary basins distributed over a prolonged depression with around 250 km and NE-trending, almost parallel to the coastline (Riccomini 1989; Riccomini et al. 2004). The Taubaté Basin is the largest of the Tertiary basins having about 170 km long, 20 km wide, and 800–850 m sedimentary thickness according to seismic profiles and gravimetric data (Fernandes and Chang 2002; Mendonça Filho et al. 2010; Carvalho et al. 2011). The Taubaté Basin is a pull-apart basin formed during the Palaeogene due to left-lateral transtension with the NE-SW trend, which reactivated during the Neogene (after quiescence period from Oligocene to Early Miocene) under right-lateral transpression with E-W trend (Cogné et al. 2013). Continental sediments fill the Tabaté Basin, where coarse granulometric sedimentary deposits are at the basin fault edges, and sandy and clay deposits, associated with fluvial-lacustrine environments, occur in the central portion (Riccomini 1989). The Precambrian crystalline basement consists of the banded gneisses and migmatites, which establish the Ribeira Fold Belt, a complex orogenic belt formed during the Pan-African assembly of the Gondwana Supercontinent (Valeriano et al. 2011). Geomorphological features of the Middle VRPS correspond to geological units formed by hills (crystalline basement) and river valley (continental sediments from the Taubaté Basin) (Ross and Moroz 1997). The relief varies from flat to gently rolling hills, with altitudes between 400 and 500 m.

The natural vegetation of Jacareí municipality restricts to Atlantic Forest fragments in the mountainous areas separated by vast pastures. The grazing areas extend along the valley between the Coast Range and the lowlands of Mantiqueira.

Materials and methods

Digital photographs and orthophotos

We used digital photographs and orthophotos from the Aerophotogrammetric Survey of the São Paulo State, developed by the "Empresa Paulista de Planejamento Metropolitano" (EMPLASA) in the years 2010/2011 (available through the license agreement number 024/15). In the study area, the acquisition date of the aerophotographs was November 7, 2011. The aerophotogrammetric survey used Ultracam cameras (X and XP models) (Scholz and Gruber 2009), which generated digital color aerial images (RGB composition) with 0.45 m resolution. The photo survey considered 60% forward overlap and 30% lateral overlap. Each photo had a corresponding metadata file containing aerotriangulation information. The EMPLASA generated digital orthophotos with 1 m resolution.

Pre- and post-urbanization digital model

The reconstruction of the pre-erosion surface using interpolation techniques for the removal of gully features in DEMs is a technique widely used to quantify the volume of eroded material (Bergonse and Reis 2015; Buccolini et al. 2012; Evans and Lindsay 2010; Perroy et al. 2010). In this research, the reconstruction of the past environment is without the presence of erosions and urban structures, being different from the investigation done in natural and rural settings.

The elaboration of the Digital Surface Model (DSM) used the MATCH-T DSM module of the Trimble INPHO commercial software based on an automatic and sequential multi-image matching method in several scales, combining feature-based and least-squares matching (Lemaire 2008). This software has been widely used by the scientific community (Gülch 2009; Höhle 2009; Costantino and Angelini 2011). However, the DSM contains natural vegetation and built features on the Earth's surface. The preparation of the pre- and post-urbanization DEMs used the techniques of filtering and extracting objects from the DSM, which are available in DTMaster software (Heuchel et al. 2011). The DTMaster tolls enable three-dimensional visualization of the point clouds and their changes while continuing to edit (Fig. 2). In the post-urbanization model, the correction of the drainage network, lake, and street errors in the DSM utilized the interpolation of digitized lines at ground level. The topological revision of the vectors eliminated errors in lines, points, and polygons such as overlap, the absence of connectivity, intersection, among others. The post-urbanization model maintained the constructions (houses, buildings, streets, among others) and eliminated the woody vegetation. Other studies to obtain the Digital Terrain Models (DTM) in forest areas and to estimate canopy height used DTMaster software (e.g., Granholm et al. 2017; Piermattei et al. 2018). Differently, the pre-urbanization model removed non-ground objects, reaching the bare ground. In this case, the interpolation considered the digitized lines parallel to the streets at ground level, eliminating the urban elements by the altimetry of the roads (Fig. 2b). Smoothing the ravines prevented the influence of urban features in the pre-urbanization flow model.

Pre- and post-urbanization differencing using contributing area and topographic indices

In the gully analysis, we used the following terrain attributes: A; W; P; and CTI. The elaboration of the A attribute used the D-infinity method (Tarboton 1997). The application of the logarithmic function (base 10) in this attribute facilitated the surface flow visualization. Many surveys for the prediction and localization of gullies used the relationship between slope (S) and A (Desmet et al. 1999; Moore et al. 1988), considering a division or multiplication operation. The W index (Beven and Kirkby 1979; O'Loughlin 1986), widely applied to soil saturation, performs a division operation expressed by:

$$W = \ln(A/\tan S). \quad (1)$$

In contrast, the P indicates the erosive power (flow intensity) or the incise capacity of the runoff (Moore et al. 1988), which establishes a multiplicative relationship defined as:

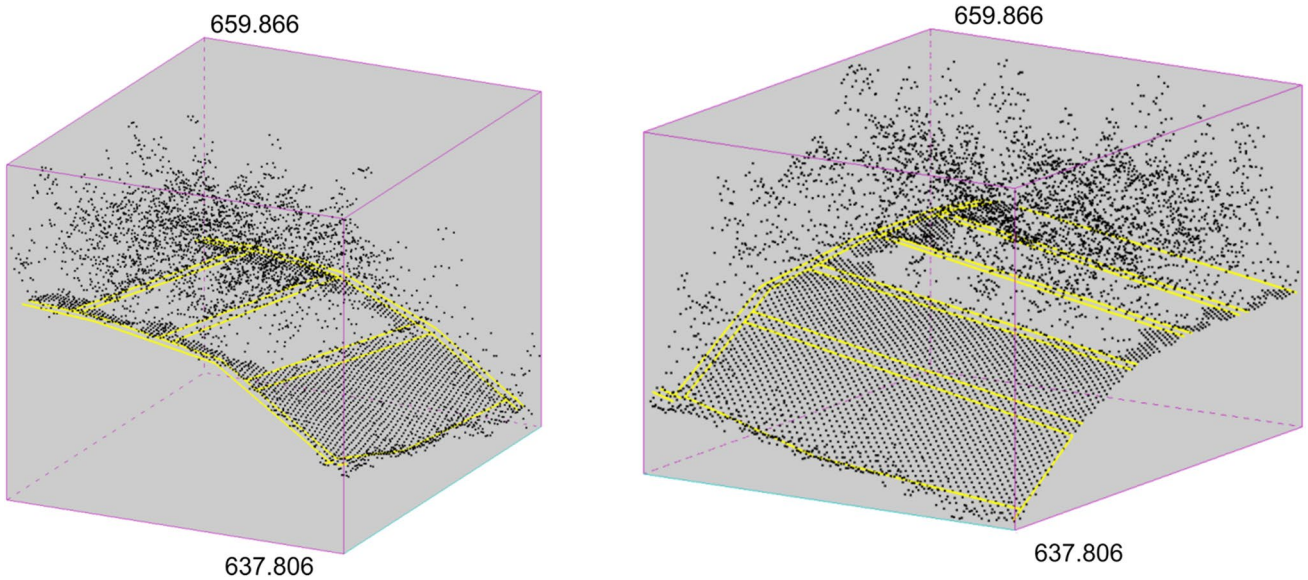

Fig. 2 Block diagram containing the cloud of elevation points from stereophotogrammetric methods, evidencing the filtering process with the elimination of artifacts above the surface

$$P = A \tan(S). \quad (2)$$

In this research, we applied the Napierian logarithmic function for the P index to decrease the data variations, highlighting runoff features. The CTI adds the planform curvature (PC) in the multiplicative expression from the following equation (Thorne et al. 1986; Zevenbergen and Thorne 1987):

$$\mathrm{CTI} = A \times S \times \mathrm{PC}. \quad (3)$$

The planform curvature is the terrain curvature perpendicular to the highest change in the slope gradient (Zevenbergen and Thorne 1987). In the bibliography, other names are suggested for the planform curvature, such as the term tangential curvature (Mitasova and Hofierka 1993; Schmidt et al. 2003) and plan curvature used in Arc/Info for the Zevenbergen and Thorne's equations (Rana 2006). The planform curvature represents the degree of convergence (concave) or divergence (convex) of the terrain, where the converging profile concentrates and accelerates the flow (Moore and Burch, 1986; Mitasova et al., 1996). According to Momm et al. (2013), a normalization of CTI values is to disregard the negative planform curvature (ridges) and apply a logarithmic function only to the pixels containing positive CTI values that are possible locations for gully initiation. Similarly, we proposed a normalized CTI ($\mathrm{CTI_n}$) by the formulation:

$$\mathrm{CTI}_n = \ln(\mathrm{abs}(\mathrm{CTI})) \times b, \quad (4)$$

where

$$b = \mathrm{CTI}/\mathrm{abs}(\mathrm{CTI}). \quad (5)$$

The "b" term establishes different signals for the concave (+ 1) and convex (− 1) areas. Finally, the application of the difference (post-urbanization minus pre-urbanization) sought to emphasize the changes of the topographic indices and their implications in triggering the erosions.

Results and discussion

Pre- and post-urbanization models

Stereophotogrammetric analysis of the DEM datasets in the DTMaster software package allowed us to reconstruct the elevation of the ground surface from the DSM. Figure 3a, b demonstrates the DSM with the elimination of above-surface features from human-made objects and forest vegetation, generating a topography that shows the natural drainage without anthropic interference. Complementarily, the visualization of three-dimensional models of contour lines (Fig. 3c, d) and surfaces (Fig. 3e, f) illustrated the result of the filtering process. The reconstructed three-dimensional model obtained continuous level contours consistent with the watershed configuration (Fig. 3d and f).

Comparison between the pre- and post-urbanization DEMs revealed a significant change in the elevation data (Fig. 4a, b). Pre-urbanization topography resulted in a smoothed DEM, removing urban and vegetation features. Meanwhile, post-urbanization topography also eliminated forest features but preserved and corrected urban elements with caution in restoring roads, which became runoff routes. Therefore, urban environments were particularly vulnerable to elevation change because of the interaction of streets, houses, buildings, and other urban features on landscape configuration. The maximum altitude in the pre-urban model was of 664 m, while in the post-urban model was of 671 m due to the values with the elevations of urban elements such as buildings. The topographic profiles became more apparent the differences between the models, with the urban model emphasized the differences among building areas and street level (Figs. 4c, d).

Geomorphic attributes

Figure 5 shows the results of the contributing area attribute and topographic indices from the pre- and post-urbanization models. In the pre-urbanization contributing area map, the runoff had a diffuse behavior with flow concentration only in the main drainages (Fig. 5a). In contrast, the post-urbanization contributing area map showed a higher flow concentration in the streets (Fig. 5b). The built-up areas inside the blocks acted as drainage dividers directing the flow to the streets, which function as channels that concentrated the surface water flow. In this context, the corrections of the surface flow routing on the natural (drainage network) and urban (highways, roads, and streets) environments were essentials in the elaborations of the DEMs, directly influencing the terrain attributes and indices. The urban surface model was challenging because of the topographically complex environment, being possible on the same street to change the flow direction. Thus, the comparison of the contributing area maps highlighted the profound changes caused by urbanization in the surface flow dynamics.

In the study area, only the drainage channels or streets concentrated significant W, ln (P), and $\mathrm{CTI_n}$ values due to the high contributing area values (Fig. 5). Outside the drainage channels, the W index highlighted a general pattern with lower values in the plateau edges and higher values in the flat areas such as the plateau and valley bottom (Fig. 5c, d). In these localities, the P index showed an inverse behavior with higher values in the plateau edges and lower values in the flat areas (Fig. 5e, f). These variations were more visible in the pre-urbanization model, because of the lack of striking urban features that imposed

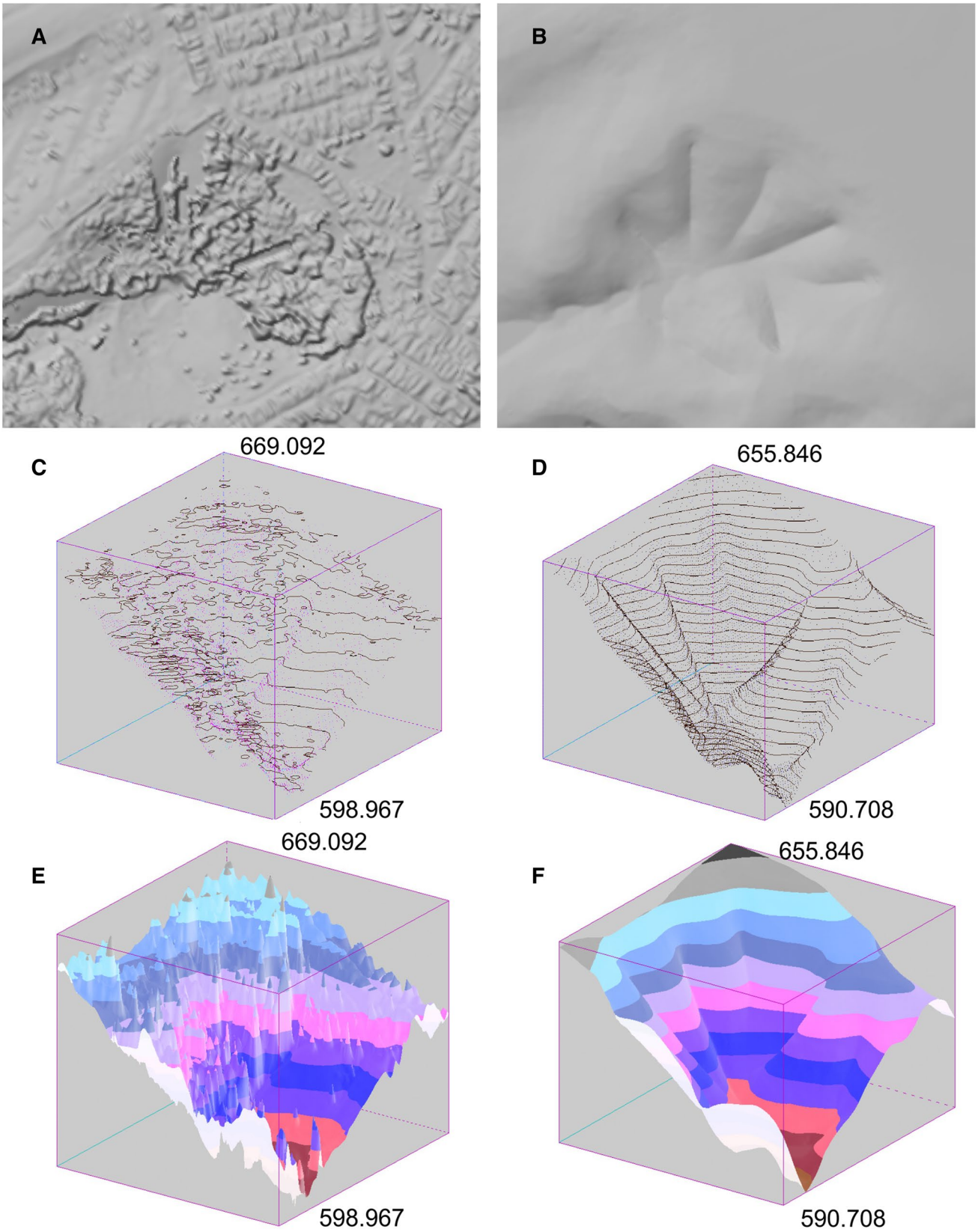

Fig. 3 Shaded relief of the digital surface model (DSM) from stereoscopic aerial photographs (**a**); digital terrain model (DTM) with a separation of above-surface features (**b**); block diagram with the DSM contour line (**c**); and block diagram of the DTM contour line (**d**)

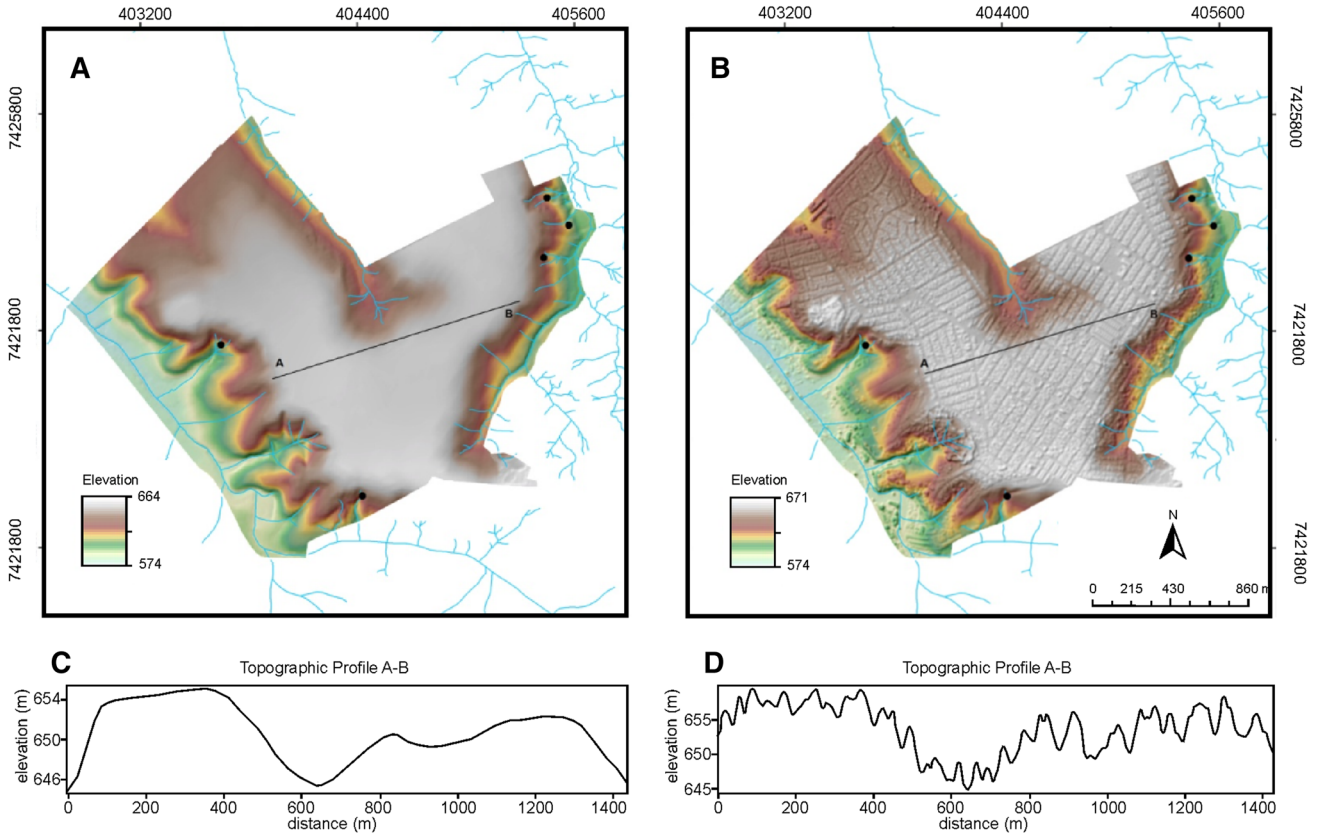

Fig. 4 **a** Pre-urbanization DEM; **b** post-urbanization DEM; **c** topographic profile from pre-urbanization DEM; and **d** topographic profile from post-urbanization

the flow along the streets (Fig. 5c and e). This spatial configuration of the *W* index, with higher values in the watershed dividers on the flat plateaus, diverged from the contributing area attribute and the other index. Unlike, the *W* index evidenced zones of saturation, which could be source areas for runoff generation. In this perspective, the *W* index did not improve the gully detection at the plateau edges but complemented the analysis by indicating nearby saturated zones with the potential to trigger a runoff. Moreover, debris deposition zones from gullies in a diffuse downslope streaking acquired higher W values.

The CTI_n evidenced topographic convergence into hollows, fragments of hillslopes with contours concave-out from the ridge (Hack and Goodlett 1960). Shapes concave in plan control the concentrated water flow route, increasing erosion, and solifluction. Therefore, the hollows evidenced the most prone areas to erosion. The convergent relief features in the CTI_n map acquired proportionally higher values than the *P* index (Fig. 5g, h). In the urban area, the presence of the houses and constructions generated an artificial curvature that delineates the streets.

Geomorphic changes

A comparison of geomorphic changes is not a purely competitive but complementary approach since it represents different aspects of the terrain analysis. The topographic index profiles of a gully considered the pre- and post-urbanization period and the relief position proposed by Ruhe (1975): summit, shoulder, backslope, footslope, and toeslope for each topographic attribute (Fig. 6). The contributing area showed for both models increasing values from summit to footslope and decreasing in toeslope. However, the contributing area differencing (post- urbanization minus pre-urbanization) denoted a profile with reduced values between summit and footslope due to the presence in the upslope convexity of diffuse flow in the pre-urbanization model and of concentrated flow coming from the city in the post-urbanization model, which makes the difference at summit greater than at footslope (Fig. 6).

In both models, the W index showed higher values in the relief positions with a low slope (summit, footslope, and toeslope), decreasing in the backslope. In contrast, the ln

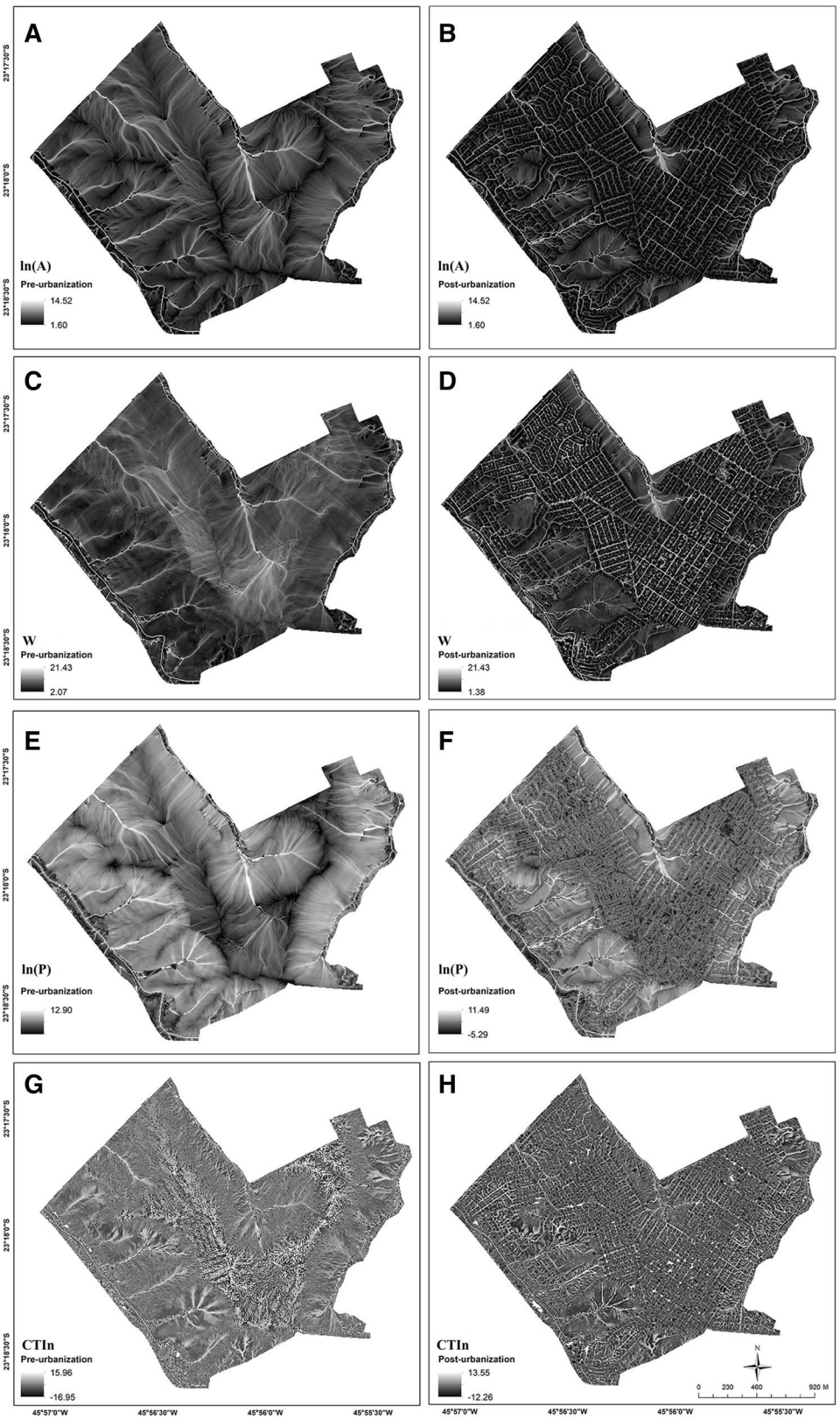

Fig. 5 Maps of topographic attributes: **a** logarithm of the contributing area (ln (*A*)) in the pre-urbanization scenario; **b** ln (*A*) in the post-urbanization scenario; **c** topographic wetness index (W) in the pre-urbanization scenario; **d** W in the post-urbanization scenario; **e** logarithm of the stream power (ln (*P*)) in the pre-urbanization scenario; **f** ln (*P*) in the post-urbanization scenario; **g** normalized compound topographic index (CTI_n) in the pre-urbanization scenario; and **h** CTI_n in the post-urbanization scenario

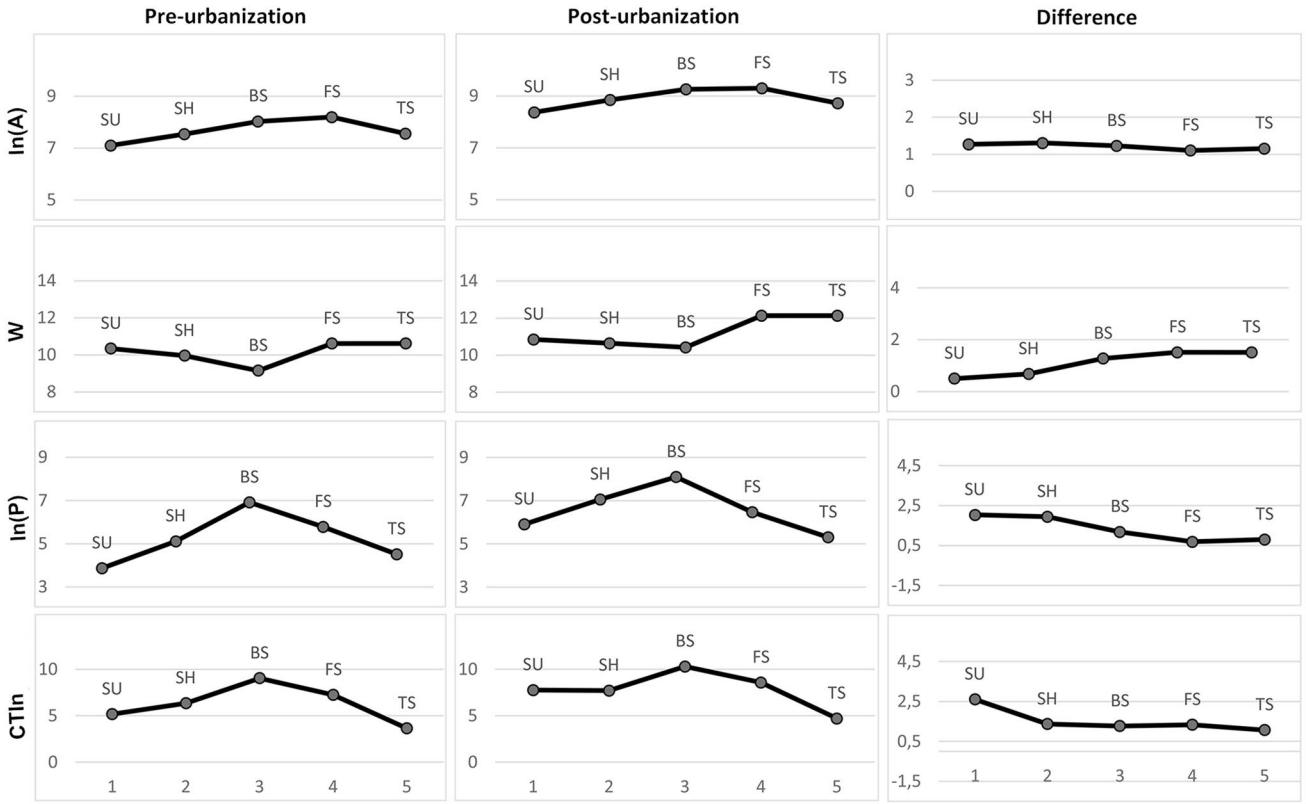

Fig. 6 Profiles of topographic indices along four gullies, considering the logarithm of the contributing area (ln (*A*)); topographic wetness index (*W*); logarithm of the stream power index (ln (*P*)); and normalized compound topographic index (CTI_n). The slope profile comprises the following landform positions: summit (SU); shoulder (SH); backslope (BS); footslope (FS), and toeslope (TS)

(*P*) index showed an inverse behavior with a higher value in the backslope position. The W and ln (*P*) differences (dW and dP) also showed an opposite response, where the dW values increased from the summit to the toeslope, while dP values decreased.

The CTI_n presented a behavior like the ln (*P*) in both scenarios, containing the highest values in the backslope due to the higher slope and concavity. The erosion process along the slope profile tended to intensify the drainage concavity, mainly in the backslope and footslope position due to the drain deepening. The difference values of CTI_n and ln (*P*) presented similarity, decreasing from the summit to the toeslope. The highest value at the summit was due to post-urbanization flow concentration. The CTI_n points of the gullies and non-gullies showed the largest distance between the indices.

In the study area, the presence of urban structures significantly modified the landscape and triggered the appearance of five gullies (Fig. 7). These urban gullies were likely a result of a combination of factors related to both natural and anthropogenic processes, which interact to increase the concentration of surface water flow and its erosive effect. The development of gullies occurs in areas adjacent to urban settlements when the rainwater concentration increases in the built area due to the lack or insufficiency of the rainwater sewage system and reaches peri-urban areas. During heavy tropical rainfall, storm sewer systems may not capture all the runoff, causing ravines in the natural drainage channels connected to the discharge of water from urban surfaces. Figure 7 shows a scatterplot comparing the behavior of topographic indices between pre- versus post-urbanization for gullied and ungullied sites. In the gully site, there is a significant increase of contributing area and topographic indices from the pre-urbanization condition to the post-urbanization, evidencing the runoff-concentration effect from the city's streets to drainages on the outskirts of the built-up areas. On the other hand, ungullied sites showed lower topographic indices with the urbanization.

Comparison of results with other researches

Diverse researches show the soil erosion is a major environmental problem in the rapid urban expansion (Lu et al. 2015; Wang et al. 2018). Changes in water flux either because of human activities (such as urbanization) or natural (climate change driven extreme flood events) are mainly driving

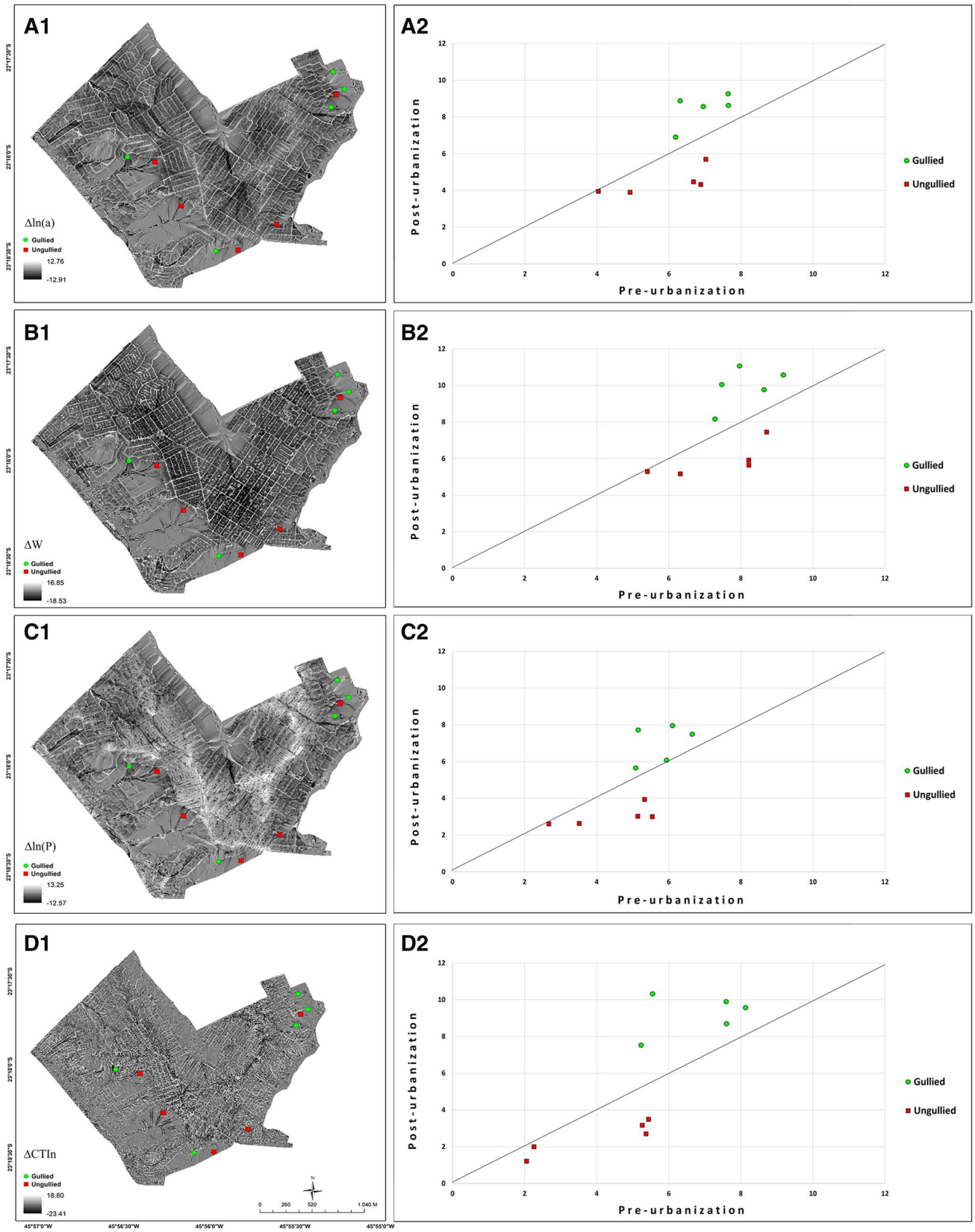

Fig. 7 Pre- and post-urbanization difference maps and their respective scatter plots in gullied (circles) and ungullied (squares) locations, considering the following attributes: **a** logarithm of the contributing area, **b** topographic wetness index; **c** logarithm of the stream power index; and **d** normalized compound topographic index

erosion risk. In Brazil, the two factors are combined, having a tropical climate that favors the presence of heavy rains in the summer season and many cities with a disorderly urban expansion (Zuquette et al. 2004; Xavier et al. 2019).

The urbanization process replaces natural areas with impermeable surfaces that reduce the amount of groundwater recharge and increase the runoff. The results of this research are consistent with other studies that observed the intensification of erosion instability from the concentrated runoff at the road surface, establishing threshold values for the contributing area and slope (Montgomery 1994; Imwangana et al. 2014). The backslope for being in steep areas presented an intense erosive action, containing the highest values of P and CTI_n. According to (Conforti et al. 2011), the susceptibility to gully erosion is strong control by the P factor. Kakembo et al. (2009) demonstrated the predisposition of abandoned lands to gully erosion using the P index.

Most studies of geomorphic changes in the gully system occurred in natural or rural settings (Aucelli et al. 2016, Betts et al. 2003), with few studies in urban environments. The results obtained by Junior (2010), restricted to the change detection of contributing areas, were compatible with those found in this study. The spatial analysis of the gullies in the study area showed that the road network was a conditioning factor for the concentration of water and erosion development. Therefore, the methods evaluated provide the spatial pattern of surface water flux change and its associated erosive processes, but these methods have limitations for accurate quantification requiring more effective field methods.

Conclusions

The results of this investigation demonstrate a strong relationship between urbanization and erosion processes. The urban morphology causes changes in the flow and volume of water that accentuate the erosive process around the built urban areas. In the evaluation of urban outflow from the digital elevation model, streets and their flow directions should be detailed, not requiring the definition of discrete and geometrically accurate objects such as walls and roofs of buildings. The geomorphological and hydrological change detections from the pre- and post-urbanization measures provide a description of the rerouting and an order of magnitude of the water volume changes, identifying the locations with the potential for accelerated erosion. In the study area, the urban intervention led to a concentration of flow along the slopes that causes instability in the landscape and accelerated erosion. The topographic indices have a complementarity, where ln (P) and CTI_n highlights the backslope, ln (A) evidences the footslope, and W the footslope and toeslope. Understanding the geomorphic changes by urbanization is essential for the automated identification of gully initiation points in the peri-urban areas, allowing the establishment of strategies for the improvement of urban drainage and watershed conservation. Despite their significant potential in urban erosion studies, few types of research use the geomorphic changes for urban environments and should be further explored.

Acknowledgements The authors are thankful to the financial support from CNPq fellowship (Osmar Abílio de Carvalho Júnior, Renato Fontes Guimarães, and Roberto Arnaldo Trancoso Gomes). Special thanks are given to the "Empresa de Planenjamento e Logística" (EPL) for additional support.

References

Adediji A, Jeje LK, Ibitoye MO (2013) Urban development and informal drainage patterns: gully dynamics in Southwestern Nigeria. Appl Geogr 40:90–102. https://doi.org/10.1016/j.apgeog.2013.01.012

Angel S, Parent J, Civco DL, Blei A, Potere D (2011) The dimensions of global urban expansion: estimates and projections for all countries, 2000–2050. Prog Plan 75:53–107. https://doi.org/10.1016/j.progress.2011.04.001

Archibold OW, Levesque LMJ, De Boer DH, Aitken AE, Delanoy L (2003) Gully retreat in a semi-urban catchment in Saskatoon. Sask Appl Geogr 23(4):261–279. https://doi.org/10.1016/j.apgeog.2003.08.005

Aucelli PP, Conforti M, Della Seta M, Del MonteD'uva ML, Rosskopf CM, Vergari F (2016) Multi-temporal digital photogrammetric analysis for quantitative assessment of soil erosion rates in the Landola catchment of the Upper Orcia Valley (Tuscany Italy). Land Degrad Dev 27:1075–1092. https://doi.org/10.1002/ldr.2324

Balaguer-Puig M, Marqués-Mateu Á, Lerma JL, Ibáñez-Asensio S (2018) Quantifying small-magnitude soil erosion: geomorphic change detection at plot scale. Land Degrad Dev 29(3):825–834. https://doi.org/10.1002/ldr.2826

Balaguer-Puig M, Marqués-Mateu Á, Lerma JL, Ibáñez-Asensio S (2017) Estimation of small-scale soil erosion in laboratory experiments with structure from motion photogrammetry. Geomorphology 295:285–296. https://doi.org/10.1016/j.geomorph.2017.04.035

Bergonse R, Reis E (2015) Reconstructing pre-erosion topography using spatial interpolation techniques: a validation-based approach. J Geog Sci 25(2):196–210. https://doi.org/10.1007/s11442-015-1162-2

Bouchnak H, Sfar Pelfoul M, Boussema MR, Snare MH (2009) Slope and rainfall effect on the volume of sediment yield by gully erosion in the Souar lithologic formation (Tunisia). CATENA 78:170–171. https://doi.org/10.1016/j.catena.2009.04.003

Buccolini M, Coco L, Cappadonia C, Rotigliano E (2012) Relationships between a new slope morphometric index and calanchi erosion in northern Sicily Italy. Geomorphology 149:41–48. https://doi.org/10.1016/j.geomorph.2012.01.012

Burns D, Vitvar T, McDonnell J, Hassett J, Duncan J, Kendall C (2005) Effects of suburban development on runoff generation in the Croton River basin, New York USA. J Hydrol 311(1):266–281. https://doi.org/10.1016/j.jhydrol.2005.01.022

Carrivick JL, Smith MW (2019) Fluvial and aquatic applications of structure from motion photogrammetry and unmanned aerial vehicle/drone technology. Wiley Interdiscip Rev Water 6(1):e1328. https://doi.org/10.1002/wat2.1328

Carvalho AMA, Vidal AC, Kiang CH (2011) Delimitação do embasamento da bacia de Taubaté. Geologia USP Série Científica 11(1):19–32. https://doi.org/10.5327/Z1519-874X2011000100002

Carvalho Júnior OA, Guimarães RF, Montgomery DR, Gillespie AR, Trancoso Gomes RA, Martins ES, Silva NC (2013) Karst depression detection using ASTER, ALOS/PRISM and SRTM-derived digital elevation models in the Bambuí group, Brazil. Remote Sens 6(1):330–351. https://doi.org/10.3390/rs6010330

Cavalli M, Goldin B, Comiti F, Brardinoni F, Marchi L (2017) Assessment of erosion and deposition in steep mountain basins by differencing sequential digital terrain models. Geomorphology 291:4–16. https://doi.org/10.1016/j.geomorph.2016.04.009

Cogné N, Cobbold PR, Riccomini C, Gallagher K (2013) Tectonic setting of the Taubaté Basin (southeastern Brazil): insights from régional seismic profiles and outcrop data. J S Am Earth Sci 42:194–204. https://doi.org/10.1016/j.jsames.2012.09.011

Conti JB (1975) Circulação secundária e efeito orográfico na gênese das chuvas na região les nordeste paulista. University of São Paulo, Thesis

Costa CW, Lorandi R, de Lollo JA, Imani M, Dupas FA (2018) Surface runoff and accelerated erosion in a peri-urban wellhead area in southeastern Brazil. Environ Earth Sci 77:160. https://doi.org/10.1007/s12665-018-7366-x

Deng X, Xu Y (2018) Degrading flood regulation function of river systems in the urbanization process. Sci Total Environ 622:1379–1390. https://doi.org/10.1016/j.scitotenv.2017.12.088

Deng X, Xu Y, Han L, Song S, Yang L, Li G, Wang Y (2015) Impacts of urbanization on river systems in the Taihu Region. China Water 7(4):1340–1358. https://doi.org/10.3390/w7041340

Dewan A, Corner R, Saleem A, Rahman MM, Haider MR, Rahman MM, Sarker MH (2017) Assessing channel changes of the Ganges-Padma river system in Bangladesh using Landsat and hydrological data. Geomorphology 276:257–279. https://doi.org/10.1016/j.geomorph.2016.10.017

Duffy JP, Shutler JD, Witt MJ, DeBell L, Anderson K (2018) Tracking fine-scale structural changes in coastal dune morphology using kite aerial photography and uncertainty-assessed structure-from-motion photogrammetry. Remote Sens 10(9):1494. https://doi.org/10.3390/rs10091494

Eltner A, Maas HG, Faust D (2018) Soil micro-topography change detection at hillslopes in fragile Mediterranean landscapes. Geoderma 313:217–232. https://doi.org/10.1016/j.geoderma.2017.10.034

Evans M, Lindsay J (2010) High resolution quantification of gully erosion in upland peatlands at the landscape scale. Earth Surf Proc Land 35(8):876–886. https://doi.org/10.1002/esp.1918

Fernandes FL, Chang HK (2001) Modelagem gravimétrica da bacia de Taubaté: vale do rio Paraíba do Sul, leste do estado de São Paulo. Br J Geophys 19:131–144. https://doi.org/10.1590/S0102-261X2001000200002

Flörke M, Schneider C, McDonald RI (2018) Water competition between cities and agriculture driven by climate change and urban growth. Nat Sustain 1(1):51–58. https://doi.org/10.1038/s41893-017-0006-8

Frankl A, Nyssen J, De Dapper M, Haile M, Billi P, Munro RN, Deckers J, Poesen J (2011) Linking long term gully and river channel dynamics to environmental change using repeat photography (Northern Ethiopia). Geomorphology 129:238–251. https://doi.org/10.1016/j.geomorph.2011.02.018

Frankl A, Stal C, Abraha A, Nyssen J, Rieke-Zapp D, De Wulf A, Poesen J (2015) Detailed recording of gully morphology in 3D through image-based modelling. CATENA 127:92–101. https://doi.org/10.1016/j.catena.2014.12.016

Glendell M, McShane G, Farrow L, James MR, Quinton J, Anderson K, Evans M, Benaud P, Rawlins B, Morgan D, Jones L, Kirkham M, DeBell L, Quine TA, Lark M, Rickson J, Brazier RE (2017) Testing the utility of structure-from-motion photogrammetry reconstructions using small unmanned aerial vehicles and ground photography to estimate the extent of upland soil erosion. Earth Surf Proc Land 42(12):1860–1871. https://doi.org/10.1002/esp.4142

Gómez-Gutiérrez A, Schnabel S, Berenguer-Sempere F, Lavado-Contador F, Rubio-Delgado J (2014) Using 3D photo-reconstruction methods to estimate gully headcut erosion. CATENA 120:91–101. https://doi.org/10.1016/j.catena.2014.04.004

Goodwin NR, Armston JD, Muir J, Stiller I (2017) Monitoring gully change: a comparison of airborne and terrestrial laser scanning using a case study from Aratula, Queensland. Geomorphology 282:195–208. https://doi.org/10.1016/j.geomorph.2017.01.001

Granholm AH, Lindgren N, Olofsson K, Nyström M, Allard A, Olsson H (2017) Estimating vertical canopy cover using dense image-based point cloud data in four vegetation types in southern Sweden. Int J Remote Sens 38(7):1820–1838. https://doi.org/10.1080/01431161.2017.1283074

Grimm NB, Faeth SH, Golubiewski NE, Redman CL, Wu J, Bai X, Briggs JM (2008) Global change and the ecology of cities. Science 319(5864):756–760. https://doi.org/10.1126/science.1150195

Grove JR, Thompson CJC (2013) Quantifying different riverbank erosion processes during an extreme flood event. Earth Surf Proc Land 38(12):1393–1406. https://doi.org/10.1002/esp.3386

Guisado-Pintado E, Jackson DW, Rogers D (2019) 3D mapping efficacy of a drone and terrestrial laser scanner over a temperate beach-dune zone. Geomorphology 328:157–172. https://doi.org/10.1016/j.geomorph.2018.12.013

Güneralp I, Rhoads BL (2009) Empirical analysis of the planform curvature-migration relation of meandering rivers. Water Resour Res 45(9):W09424. https://doi.org/10.1029/2008WR007533

Gupta A (2002) Geoindicators for tropical urbanization. Environ Geol 42(7):736–742. https://doi.org/10.1007/s00254-002-0551-x

Gurnell A, Lee M, Souch C (2007) Urban rivers: hydrology, geomorphology, ecology, and opportunities for change. Geogr Compass 1(5):1118–1137. https://doi.org/10.1111/j.1749-8198.2007.00058.x

Hack JT, Goodlett JC (1960) Geomorphology and forest ecology of a mountain region in the central Appalachians. Prof Pap 347:1–66. https://doi.org/10.3133/pp347

Heuchel T, Köstli A, Lemaire C, Wild D (2011) Towards a next level of quality DSM/DTM extraction with Match-T. In: Fritsch D (ed) 53rd proceedings of photogrammetric week. Herbert Wichmann Verlag, Stuttgart, Germany, pp 197–202

Hsieh YC, Chan YC, Hu JC (2016) Digital elevation model differencing and error estimation from multiple sources: a case study from the Meiyuan Shan landslide in Taiwan. Remote Sens 8(3):199. https://doi.org/10.3390/rs8030199

Imwangana FM, Dewitte O, Ntombi M, Moeyersons J (2014) Topographic and road control of mega-gullies in Kinshasa (DR Congo). Geomorphology 217:131–139. https://doi.org/10.1016/j.geomorph.2014.04.021

IPEADATA (2018) https://www.ipeadata.gov.br/. Accessed 05 February 2018

Jeong A, Dorn RI (2019) Soil erosion from urbanization processes in the Sonoran Desert, Arizona, USA. Land Degrad Dev 30(2):226–238. https://doi.org/10.1002/ldr.3207

Jones BM, Stoker JM, Gibbs AE, Grosse G, Romanovsky VE, Douglas TA, Kinsman NEM, Richmond BM (2013) Quantifying landscape change in an arctic coastal lowland using repeat airborne LiDAR. Environ Res Lett 8(4):045025. https://doi.org/10.1088/1748-9326/8/4/045025

Junior OC, Guimaraes RF, Freitas L, Gomes-Loebmann D, Gomes RA, Martins E, Montgomery DR (2010) Urbanization impacts upon catchment hydrology and gully development using

mutli-temporal digital elevation data analysis. Earth Surf Proc Land 35:611–617. https://doi.org/10.1002/esp.1917
Kakembo V, Xanga WW, Rowntree K (2009) Topographic thresholds in gully development on the hillslopes of communal areas in Ngqushwa Local Municipality, Eastern Cape. S Af Geomorphol 110(3–4):188–194. https://doi.org/10.1016/j.geomorph.2009.04.006
Kasprak A, Bransky ND, Sankey JB, Caster J, Sankey TT (2019) The effects of topographic surveying technique and data resolution on the detection and interpretation of geomorphic change. Geomorphology 333:1–15. https://doi.org/10.1016/j.geomorph.2019.02.020
Kobal M, Bertoncelj I, Pirotti F, Dakskobler I, Kutnar L (2015) Using Lidar data to analyse sinkhole characteristics relevant for understory vegetation under forest cover—case study of a high karst area in the Dinaric Mountains. PLoS ONE 10(3):e0122070. https://doi.org/10.1371/journal.pone.0122070
Le Mauff B, Juigner M, Ba A, Robin M, Launeau P, Fattal P (2018) Coastal monitoring solutions of the geomorphological response of beach-dune systems using multi-temporal LiDAR datasets (Vendée coast, France). Geomorphology 304:121–140. https://doi.org/10.1016/j.geomorph.2017.12.037
Lu Q, Gao Z, Ning J, Bi X, Wang Q (2015) Impact of progressive urbanization and changing cropping systems on soil erosion and net primary production. Ecol Eng 75:187–194. https://doi.org/10.1016/j.ecoleng.2014.11.048
Marengo JA, Alves LM (2005) Tendências hidrológicas da bacia do rio Paraíba do Sul. Rev Bras Meteorol 20(2):215–226
Martínez-Casasnovas JA, Ramos MC, Garcìa-Hernàndez D (2009) Effects of land-use changes in vegetation cover and sidewall erosion in a gully head of the Penedès region (northeast Spain). Earth Surf Proc Land 34:1927–1937. https://doi.org/10.1002/esp.1870
Mejía AI, Moglen GE (2010) Spatial distribution of imperviousness and the space-time variability of rainfall, runoff generation, and routing. Water Resour Res 46(7):W07509. https://doi.org/10.1029/2009WR008568
Mendonça Filho JG, Chagas RBA, Menezes TR, Mendonça JO, da Silva FS, Sabadini-Santos E (2010) Organic facies of the Oligocene lacustrine system in the Cenozoic Taubaté basin, Southern Brazil. Int J Coal Geol 84:166–178. https://doi.org/10.1016/j.coal.2010.07.004
Micheletti N, Tonini M, Lane SN (2017) Geomorphological activity at a rock glacier front detected with a 3D density-based clustering algorithm. Geomorphology 278:287–297. https://doi.org/10.1016/j.geomorph.2016.11.016
Mitasova H, Hofierka J (1993) Interpolation by regularized spline with tension: II application to terrain modeling and surface geometry analysis. Math Geol 25:657–669. https://doi.org/10.1007/BF00893172
Mitasova H, Hofierka J, Zlocha M, Iverson L (1996) Modeling topographic potential for erosion and deposition using GIS. Int J Geogr Inf Syst 10(5):629–641. https://doi.org/10.1080/02693799608902101
Momm HG, Bingner RL, Wells RR, Rigby JR, Dabney SM (2013) Effect of topographic characteristics on compound topographic index for identification of gully channel initiation locations. Trans ASABE 56(2):523–537. https://doi.org/10.13031/2013.42673
Montgomery DR (1994) Road surface drainage, channel initiation, and slope instability. Water Resour Res 30(6):1925–1932. https://doi.org/10.1029/94WR00538
Moore ID, Burch GJ, Mackenzie DH (1988) Topographic effects on the distribution of surface soil water and the location of ephemeral gullies. Trans ASAE 31(4):1098–1107. https://doi.org/10.13031/2013.30829
Moore ID, Burch GJ (1986) Modeling erosion and deposition: topographic effects. Trans Am Soc Agric Eng 29:1624–1640. https://doi.org/10.13031/2013.30363
Mora O, Lenzano M, Toth C, Grejner-Brzezinska D, Fayne J (2018) Landslide change detection based on multi-temporal Airborne LiDAR-derived DEMs. Geosciences 8(1):23. https://doi.org/10.3390/geosciences8010023
Norman LM, Sankey JB, Dean D, Caster J, DeLong S, DeLong W, Pelletier JD (2017) Quantifying geomorphic change at ephemeral stream restoration sites using a coupled-model approach. Geomorphology 283:1–16. https://doi.org/10.1016/j.geomorph.2017.01.017
Nuth C, Kääb A (2011) Co-registration and bias corrections of satellite elevation data sets for quantifying glacier thickness change. Cryosphere 5(1):271–290. https://doi.org/10.5194/tc-5-271-2011
Oskin ME, Arrowsmith JR, Corona AH, Elliott AJ, Fletcher JM, Fielding EJ, Gold PO, Garcia JJG, Hudnut KW, Liu-Zeng J, Teran OJ (2012) Near-field deformation from the El Mayor-Cucapah earthquake revealed by differential LIDAR. Science 335(6069):702–705. https://doi.org/10.1126/science.1213778
Peppa MV, Mills JP, Moore P, Miller PE, Chambers JE (2019) Automated co-registration and calibration in SfM photogrammetry for landslide change detection. Earth Surf Proc Land 44(1):287–303. https://doi.org/10.1002/esp.4502
Perroy RL, Bookhagen B, Asner GP, Chadwick OA (2010) Comparison of gully erosion estimates using airborne and ground-based LiDAR on Santa Cruz Island, California. Geomorphology 118:288–300. https://doi.org/10.1016/j.geomorph.2010.01.009
Piccarreta M, Capolongo D, Miccoli MN, Bentivenga M (2012) Global change and long-term gully sediment production dynamics in Basilicata, southern Italy. Environ Earth Sci 67:1619–1630. https://doi.org/10.1007/s12665-012-1603-5
Piermattei L, Marty M, Karel W, Ressl C, Hollaus M, Ginzler C, Pfeifer N (2018) Impact of the acquisition geometry of very high-resolution Pléiades imagery on the accuracy of canopy height models over forested alpine regions. Remote Sens 10(10):1542. https://doi.org/10.3390/rs10101542
Pineux N, Lisein J, Swerts G, Bielders CL, Lejeune P, Colinet G, Degré A (2017) Can DEM time series produced by UAV be used to quantify diffuse erosion in an agricultural watershed? Geomorphology 280:122–136. https://doi.org/10.1016/j.geomorph.2016.12.003
Pribadi DO, Vollmer D, Pauleit S (2018) Impact of peri-urban agriculture on runoff and soil erosion in the rapidly developing metropolitan area of Jakarta. Indones Reg Environ Change 18(7):2129–2143. https://doi.org/10.1007/s10113-018-1341-7
Rana S (2006) Use of plan curvature variations for the identification of ridges and channels on DEM. In: Riedl A, Kainz W, Elmes GA (eds) Progress in spatial data handling. Springer, Berlin, Heidelberg, pp 789–804. https://doi.org/10.1007/3-540-35589-8_49
Ren Z, Zhang Z, Dai F, Yin J, Zhang H (2014) Topographic changes due to the 2008 Mw7.9 Wenchuan earthquake as revealed by the differential DEM method. Geomorphology 217:122–130. https://doi.org/10.1016/j.geomorph.2014.04.020
Ries JB, Marzolff I (2003) Monitoring of gully erosion in the Central Ebro Basin by large-scale aerial photography taken from a remotely controlled blimp. CATENA 50:309–328. https://doi.org/10.1016/S0341-8162(02)00133-9
Rose S, Peters NE (2001) Effects of urbanization on streamflow in the Atlanta area (Georgia, USA): a comparative hydrological approach. Hydrol Process 15(8):1441–1457. https://doi.org/10.1002/hyp.218
Ross JLS, Moroz IC (1997) Mapa Geomorfológico do Estado de São Paulo 15:000.00. DG-FFLCH-USP/IPT/Fapesp, São Paulo
Ruhe RV (1975) Geomorphology. Houghton and Mifflin Co, Boston, MA, p 246

São Paulo: Conselho Estadual de Recursos Hídricos (2006) Plano estadual de recursos hídricos 2004–2007 Resumo. Secretaria de energia, recursos hídricos e saneamento, São Paulo, Brasil. http://www.sigrh.sp.gov.br/public/uploads/documents/7006/perh.pdf

Schmidt J, Evans IS, Brinkmann J (2003) Comparison of polynomial models for land surface curvature calculation. Int J Geogr Inf Sci 17(8):797–814. https://doi.org/10.1080/13658810310001596058

Scholz S, Gruber M (2009) Radiometric and geometric quality aspects of the large format aerial camera UltraCam-Xp. In: ISPRS (ed) Proceedings of ISPRS Hannover workshop 2009: High-resolution earth imaging for geospatial information. ISPRS, Hannover, Germany, 2–5 June 2009, vol 38, pp 143–147. https://citeseerx.ist.psu.edu/viewdoc/download?doi=10.1.1.410.859&rep=rep1&type=pdf

Seier G, Kellerer-Pirklbauer A, Wecht M, Hirschmann S, Kaufmann V, Lieb GK, Sulzer W (2017) UAS-based change detection of the glacial and proglacial transition zone at Pasterze Glacier. Austria Remote Sens 9(6):549. https://doi.org/10.3390/rs9060549

Seto KC, Fragkias M, Güneralp B, Reilly MK (2011) A meta-analysis of global urban land expansion. PLoS ONE 6:e23777. https://doi.org/10.1371/journal.pone.0023777

Shukla S, Gedam S (2019) Evaluating hydrological responses to urbanization in a tropical river basin: a water resources management perspective. Nat Resour Res 28(2):327–347. https://doi.org/10.1007/s11053-018-9390-7

Siart C, Bubenzer O, Eitel B (2009) Combining digital elevation data (SRTM/ASTER), high resolution satellite imagery (Quickbird) and GIS for geomorphological mapping: a multi-component case study on Mediterranean karst in Central Crete. Geomorphology 112:106–121. https://doi.org/10.1016/j.geomorph.2009.05.010

Taniguchi KT, Biggs TW, Langendoen EJ, Castillo C, Gudino-Elizondo N, Yuan Y, Liden D (2018) Stream channel erosion in a rapidly urbanizing region of the US–Mexico border: documenting the importance of channel hardpoints with structure-from-motion photogrammetry. Earth Surf Proc Land 43(7):1465–1477. https://doi.org/10.1002/esp.4331

Tarboton DG (1997) A new method for the determination of flow directions and upslope areas in grid digital elevation models. Water Resour Res 33(2):309–319. https://doi.org/10.1029/96WR03137

Taylor RJ, Massey C, Fuller IC, Marden M, Archibald G, Ries W (2018) Quantifying sediment connectivity in an actively eroding gully complex, Waipaoa catchment, New Zealand. Geomorphology 307:24–37. https://doi.org/10.1016/j.geomorph.2017.10.007

Thorne CR, Zevenbergen LW, Grissinger EH, Murphey JB (1986) Ephemeral gullies as sources of sediment. Proc Fourth Fed Interag Sediment Conf Las Vegas Nevada 1(3):152–161 **(March 24-27 1986)**

United Nations department of economic and social affairs population division (2015) world urbanization prospects: the 2014 revision. United Nations department of economic and social affairs population division New York https://esa.un.org/unpd/wup/publications/files/wup2014-report.pdf Accessed 31 August 2018.

Valeriano CM, Tupinambá M, Simonetti A, Heilbron M, de Almeida JCH, do Eirado LG (2011) U-Pb LA-MC-ICPMS geochronology of Cambro-Ordovician post-collisional granites of the Ribeira belt, southeast Brazil: terminal Brasiliano magmatism in central Gondwana supercontinent. J S Am Earth Sci 32(4):416–428. https://doi.org/10.1016/j.jsames.2011.03.003

Vinci A, Todisco F, Brigante R, Mannocchi F, Radicioni F (2017) A smartphone camera for the structure from motion reconstruction for measuring soil surface variations and soil loss due to erosion. Hydrol Res 48:673–685. https://doi.org/10.2166/nh.2017.075

Wang LY, Xiao Y, Rao EM, Jiang L, Xiao Y, Ouyang ZY (2018) An assessment of the impact of urbanization on soil erosion in Inner Mongolia. Int J Environ Res Pub Health 15(3):550. https://doi.org/10.3390/ijerph15030550

Xavier SC, Bressani LA (2019) Progressive mapping and urban growth: the construction of urbanization suitability map of Pelotas-Southern Brazil. Soils Rocks 42(2):99–116. https://doi.org/10.28927/SR.422099

Xiong L, Wang G, Bao Y, Zhou X, Sun X, Zhao R (2018) Detectability of repeated airborne laser scanning for mountain landslide monitoring. Geosciences 8(12):469. https://doi.org/10.3390/geosciences8120469

Zevenbergen LW, Thorne CR (1987) Quantitative analysis of land surface topography. Earth Surf Proc Land 12(1):47–56. https://doi.org/10.1002/esp.3290120107

Zolezzi G, Bezzi M, Spada D, Bozzarelli E (2018) Urban gully erosion in sub-Saharan Africa: a case study from Uganda. Land Degrad Dev 29(3):849–859. https://doi.org/10.1002/ldr.2865

Zuquette LV, Pejon OJ, dos Santos Collares JQ (2004) Land degradation assessment based on environmental geoindicators in the Fortaleza metropolitan region, state of Ceará. Braz Environ Geol 45(3):408–425. https://doi.org/10.1007/s00254-003-0892-0